Computational Project. Equilibrium Monte Carlo simulation of the 2D Ising model

Autors: *Manel Díaz, Adrián Llamas, Itxaso Muñoz*
Curs: Modelització Molecular (MoMo)
2025–2026

Barcelona, desembre 2025

Abstract

This project implements an equilibrium Markov-chain Monte Carlo simulation of the two-dimensional Ising model in the canonical ensemble, using the Metropolis single-spin-flip algorithm, with periodic boundary conditions. Time series of two observables (energy and magnetization) are generated for different lattice sizes and temperatures, with their corresponding statistical uncertainties, computed using a binning (block) analysis to account for autocorrelations. [2] The correctness of the implementation is validated by reproducing the Ferdinand-Fischer finite-size reference value for $L = 20$ at $T = 2.0$, after discarding an initial equilibration transient. [1]

1 Estimates, interpretations and comments

In this section, we include all the relevant information relative to the simulations, such as direct estimates and complemental material to the figures in Sec. 2.

1.1 Testing our code. Estimating $\langle E\rangle/L^2$. Comparison with Ferdinand-Fisher.

In order to test the correctness of our MC code, a simulation with $L = 20$, $T = 2$ and a sampling frequency of $n_{\text{meas}} = 10$ was performed, starting with random initial conditions, for a total of $n_{\text{MCS}} = 10^8$ MC steps, [1] leaving the first 10^3 steps, in order to compute the sample average $\bar{E}$ directly, yielding a value of $\bar{E} = -698.2353484\ldots$. The binning code was used to extract a statistical error of $\sigma_E(m = 128) = 3 \times 10^{-5}$, since from Fig. 1 we see that the errors do not depend on the choice of the binning sample size for $m = 128$. Therefore we obtained $\langle E\rangle/L^2 = -1.74558 \pm 3 \times 10^{-5}$ as the final estimate. Comparing this result with the *exact* value given by Ferdinand and Fisher $\langle E\rangle/L^2\big|_{\text{FF}} = -1.7455571250\ldots$ we see that the exact value lies within the obtained margin of error and thus is in agreement (up to the fifth decimal place), with a relative discrepancy of $\delta(\langle E\rangle/L^2) \approx 0.002\,\%$.

1.2 Evolution of E and M for different T. Comparison between $L = 20$ and $L = 100$.

Once the code had passed the Ferdinand-Fisher test, different production runs were done for $L = 100$ and temperatures $2 \leq T \leq 3$ every $\Delta T = 0.1$, with a particular emphasis on the $T = 2.0$, $T = 2.27$, $T = 2.6$ cases. A sampling frequency of $n_{\text{meas}} = 10$ was used and a total of $n_{\text{MCS}} = 10^8$ MC steps as well. Figures 2 and 3 show the time series for E and M, respectively, for $T = 2.0$, $T = 2.27$, $T = 2.6$.

From Fig. 2 we can see how, after the first 10^3 MC steps, the *energy* reaches stationary values, fluctuating around a well-defined average. As T increases, the system settles at decreasing (negative) values of the energy. It is worth mentioning that the time series for $T = 2.27$ the energy fluctuations become more relevant, compared with the other cases.

Fig. 3 depicts the respective time series for the *magnetization* M. At a low temperature of $T = 2$ (relative to some critical temperature T_c) the system' spins tend to align between them, producing an ordered configuration, which is reflected on the value $\langle M\rangle/N \sim -1$. For a high temperature of $T = 2.6$, we see that the stationary configuration involves random orientations of the spins, thus $\langle M\rangle/N \sim 0$. Finally, and most interestingly, at $T = 2.27$ the magnetization keeps fluctuating around all its possible values, without settling, suggesting that the system is at a critical point, i.e., a ferromagnetic-paramagnetic phase transition is taking place, with order parameter M, and thus that $T = 2.27 \equiv T_c$.

In order to compare any potential effect of changing the *scale* of the system L, Fig. 4 shows the time series for $L = 20$ and $L = 100$ at $T = 2$. From them, we can see that for $L = 20$ the magnetization stabilizes much faster. Also, in both cases the system reaches an ordered stationary state, but $\langle M\rangle/N \sim 1$ for $L = 20$, whereas $\langle M\rangle/N \sim -1$ for $L = 100$. This difference is simply due to the fact that below the critical temperature there is a spontaneous symmetry breaking and the spins align either up or down.

1.3 Extracting $\langle E\rangle$ and $\langle|M|\rangle$ with its statistical errors.

With the previous MC data, a binning code was implemented to extract expected values and statistical errors. Fig. 5 and Fig. 6 show the dependence of σ on the block size m. Finally, we can estimate the autocorrelation time for $m \gg \tau_{int,A}$ since for a generic observable A

$$\frac{s^2_{\bar{A}^m}}{s^2_{\bar{A}^1}} \simeq \tau_{int,A}, \tag{1}$$

where s^2 is the binning sample variance. [2]

1.3.1 Dependence of the autocorrelation time on temperature.

In order to obtain good enough estimates of the autocorrelation times $\tau_{int,A}$, for $T = 2$, $T = 2.6$, Eq. 1 was applied and averaged over a range of values for which we know (from binning) that the statistical

errors do not depend on m. Conversely, for $T = 2.27$, since the system exhibits critical behavior, we expect from theory that $\tau_{int,A} \to \infty$ and no particular block size will remove the time correlations; as a numerical check of this fact, the value of $\tau_{int,A}$ was computed by averaging the data points with $m \gtrsim 128$. Table 1 shows the these results. The shortest autocorrelation time occurs for $T = 2.6$, for which the thermal noise is significant enough to produce faster decorrelations between successive configurations. The opposite is observed for $T = 2$, as expected. Note that, in terms of τ, $\langle|M|\rangle$ is much more sensitive than $\langle E\rangle$ to changes in the temperature.

Table 1: Autocorrelation times of $\langle E\rangle$ and $\langle|M|\rangle$, with its statistical errors, for different temperatures.

	$\tau_{\langle E\rangle}$	$\tau_{\langle|M|\rangle}$
T=2.0	1.46±0.08	11.4±0.2
T=2.27	66±32	148±73
T=2.6	1.35±0.07	3.0±0.1

1.4 Dependence of $\langle E\rangle/L^2$ and $\langle|M|\rangle/L^2$ on T.

In figures 3 and 8, we can see the dependence on T of $\langle E\rangle/N$ and $\langle|M|\rangle/N$. For the magnetization, the behavior is as expected and commented in Fig. 3: it decreases from the unity to zero, with an abrupt fluctuation at $T_c = 2.27$, being the point with the biggest error. For the case of the energy, the concavity changes at T_c from concave to convex, though it is expected to saturate for sufficiently high temperatures (since the system is finite and has a configuration that maximizes E).

1.5 Estimating χ and c from Jackknife resampling. Dependence with T.

To estimate the per spin magnetic susceptibility $\chi = \beta(\langle M^2\rangle - \langle|M|\rangle^2)/N$ and heat capacity $c = \beta^2(\langle E^2\rangle - \langle E\rangle^2)/N$, for each temperature T, Jackknife resampling is required since the different observables are correlated, specially near the critical point. In Fig. 9 the Jackknife errors of χ and c are represented as a function of the block size m, as well as the same error for χ estimated from error propagating its definition given before, yielding

$$\sigma_\chi \approx \frac{1}{NT}\sqrt{\sigma^2_{\langle M^2\rangle} + 4\langle|M|\rangle^2\sigma^2_{\langle|M|\rangle}}\,, \tag{2}$$

which naively assumes that $\mathrm{Cov}(\langle M^2\rangle, \langle|M|\rangle) = 0$, far from being true, specially at $T_c \approx 2.27$ and thus overestimating the error.

Finally, Fig. 10 depicts the dependence of χ and c on the temperature, by extracting the central value and its error from Jackknife resampling with block sizes optimally chosen at each point (which grew as we approached T_c and decreased beyond T_c). We can see how, whereas c does not present a discontinuity (consistent with the $\alpha = 0$ critical exponent for a $2D$ Ising model), near T_c, χ diverges as $\sim |T - T_c|^\gamma$, consistent with theory.

2 Figures

In this section, we list the different figures obtained from the simulation data. For further comments and interpretations, see Sec. 1.

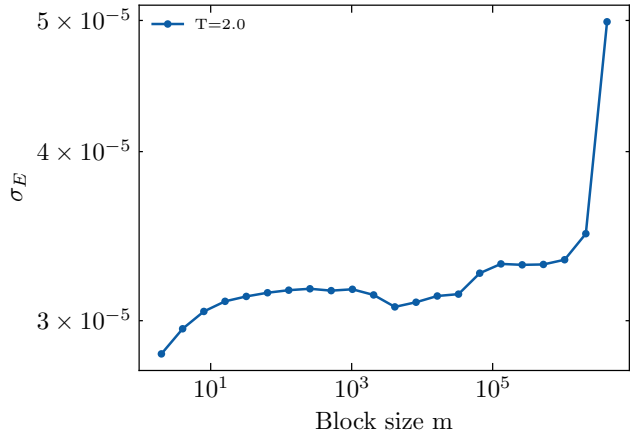

Figure 1: Statistical error (standard deviation) of the energy as a function of the block size for $L = 20$ and $T = 2.0$ in log-log scale.

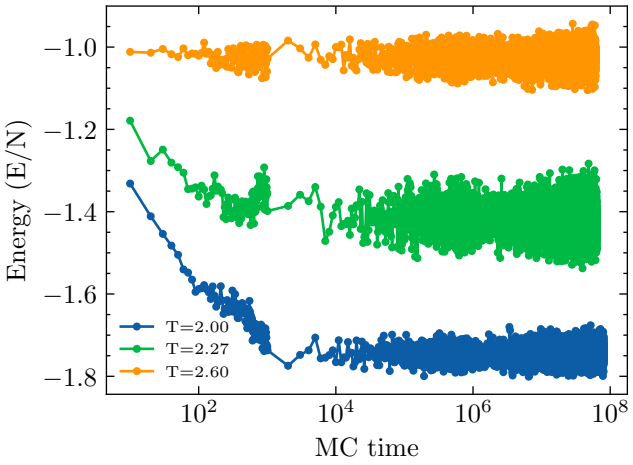

Figure 2: Energy per spin, as a function of MC time, for three temperatures, including the critical temperature, for $L = 100$.

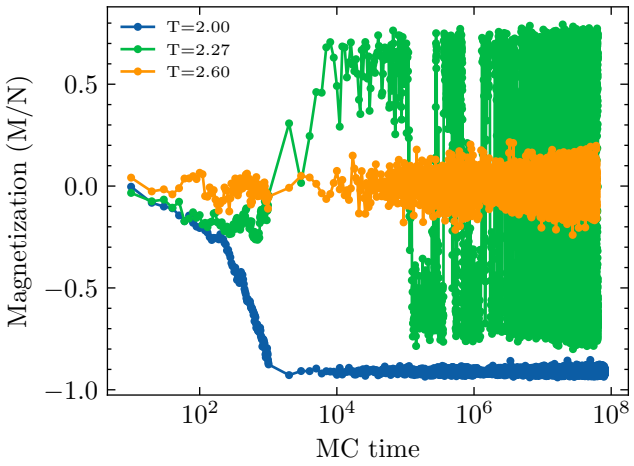

Figure 3: Magnetization per spin, as a function of MC time, for three temperatures, including the critical temperature, for $L = 100$.

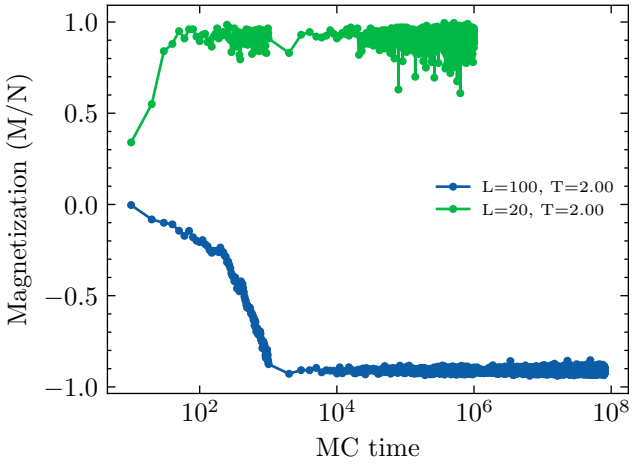

Figure 4: $T = 2$ magnetization per spin time series for $L = 20$ and $L = 100$.

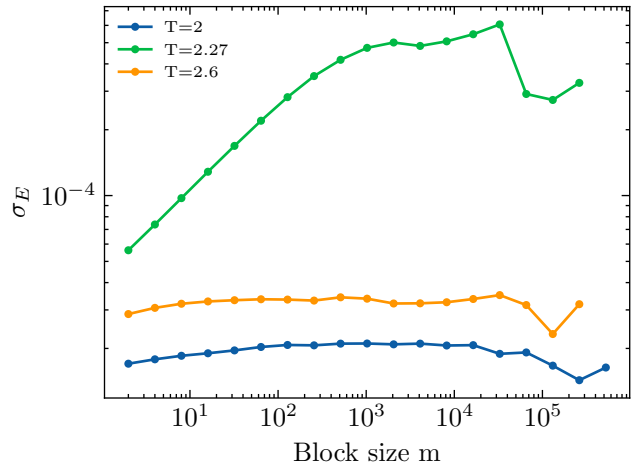

Figure 5: Statistical error (standard deviation) of the energy as a function of the block size for different temperatures, for $L = 100$ in log-log scale.

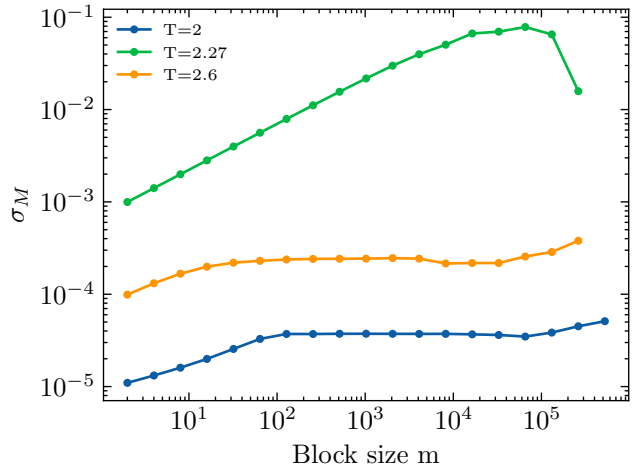

Figure 6: Statistical error (standard deviation) of the absolute value of the magnetization as a function of the block size for different temperatures for, $L = 100$ in log-log scale.

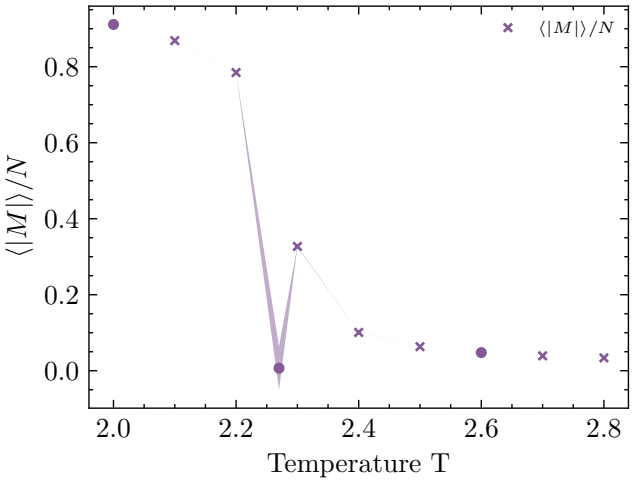

Figure 7: Average value of the absolute value of the magnetization as a function of the temperature. As dots, the requested temperatures, $T = 2.0,\ 2.27,\ 2.6$. Note that only at $T_c = 2.27$ the statistical error is greater than the data markers.

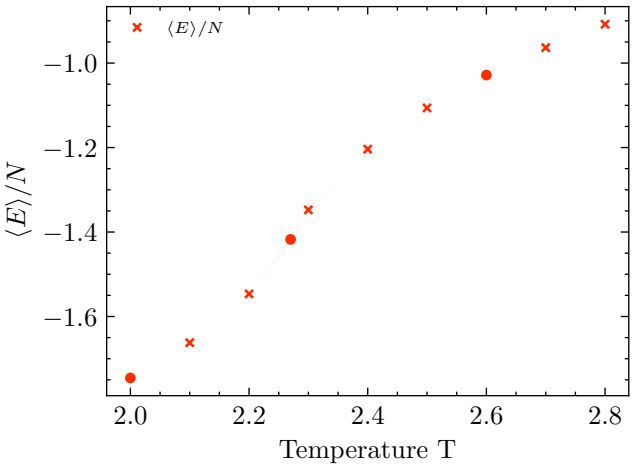

Figure 8: Average value of the energy, extracted from the binning program, as a function of the temperature. As dots, the requested temperatures, $T = 2.0, 2.27, 2.6$. The statistical errors are smaller than the data markers.

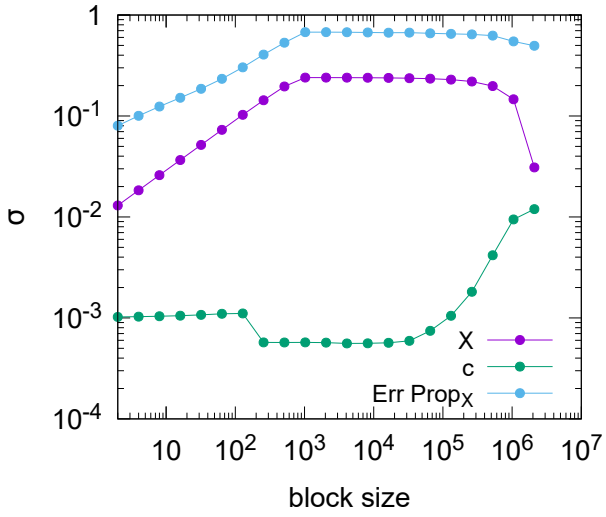

Figure 9: Log-log dependence of statistical errors on the binning block size for $L = 100$ and $T_c \approx 2.27$. The Jackknife errors for the (per spin) magnetic susceptibility χ and heat capacity c are represented in purple and green respectively. In blue is represented the error propagation for χ as well.

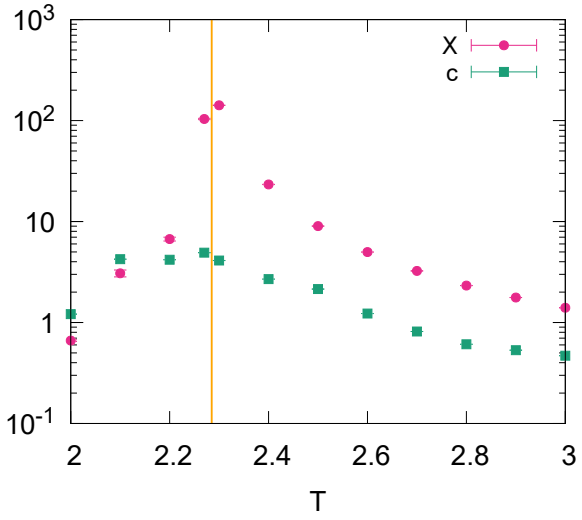

Figure 10: Semi-log per spin magnetic susceptibility χ and heat capacity c with its corresponding statistical errors for $L = 100$ and different T. In orange the critical temperature $T_c \approx 2.27$ is emphasized.

A References

References

[1] Molecular Modeling (MoMo), "Computational Project: Equilibrium Monte Carlo simulation of the 2D Ising model", academic year 2025–2026 (project statement provided on Campus Virtual; file `comp_project_2025-26.pdf`).

[2] M. Palassini, "Introduction to the Monte Carlo method", Molecular Modeling (MoMo), Fall 2025 (lecture slides provided on Campus Virtual; file `1.MASM_slides_2025-26.pdf`).

B Code: GitHub repository

`https://github.com/itxasoma/momo-McMC-2DIsing`